

# Energy, Environment and Storage

ENERGY, ENVIRONMENT STORAGE
AN INTERNATIONAL JOURNAL

Journal Homepage: www.enenstrg.com

# Investigation of the Experimental Performance of Different Savonius Wind Turbines in an Open Wind Tunnel

Burcu Hasaltın<sup>1\*</sup>, Sayra Bengü Yılmaz<sup>2</sup>, Mahmut Burak Akkuş<sup>3</sup>

<sup>1\*</sup>Erciyes University, Department of Mechanical Engineering, Kayseri, Türkiye, ORCID: 0009-0005-4927-543X <sup>2</sup>Erciyes University, Department of Mechanical Engineering, , Kayseri, Türkiye ,

<sup>3</sup>Erciyes University, Department of Mechanical Engineering, , Kayseri, Türkiye ORCID: 0000-0002-4561-7093

Abstract. This study presents a comprehensive experimental investigation into the aerodynamic performance of six Savonius wind turbine blade profiles with distinct geometries, tested systematically in an open wind tunnel facility. The motivation behind this research stems from the need to optimize small-scale wind turbines for efficient operation under low-wind-speed conditions, which are commonly encountered in urban and decentralized energy applications. To achieve this, six different blade configurations—including classical semi-cylindrical, helical, and hybrid/optimized models—were designed, fabricated, and subjected to rigorous testing. Each prototype shared identical rotor dimensions in terms of diameter and blade height, ensuring that observed differences in performance could be attributed solely to blade geometry rather than scaling effects. The experimental campaign was conducted under controlled wind conditions, with a constant free-stream wind speed, allowing for repeatability and reliability of results. Key aerodynamic performance parameters, including torque generation, rotational speed, tip speed ratio, and power coefficient, were systematically measured and analyzed. The findings clearly demonstrate that blade geometry plays a critical role in determining the overall performance of Savonius turbines. The comparative results highlight the inherent trade-offs between achieving strong initial torque and maximizing aerodynamic efficiency. These insights are particularly valuable for guiding future design improvements aimed at small-scale renewable energy systems. By demonstrating the advantages of hybrid blade designs, this study contributes to the ongoing development of compact, efficient, and reliable wind energy solutions suitable for applications in low-wind-speed regions, such as urban rooftops, agricultural fields, and off-grid installations. Ultimately, this research provides not only an experimental benchmark for Savonius turbine geometries but also practical design guidance that can inform engineers and developers in the renewable energy sector. The results serve as a foundation for further optimization studies and future innovations in the design of vertical-axis wind turbines.

Keywords: Savonius Wind Turbine Rrenewable Energy, Aerodynamic Performance.

Article History: Received:10 September 2025; Revised: 22 September 2025; Accepted:03. October 2025 Availableonline: 03 October 2025 Doi: <a href="https://doi.org/10.52924/RENW7010">https://doi.org/10.52924/RENW7010</a>

#### 1. INTRODUCTION

increasing rapidly due to climate change concerns and the depletion of fossil fuel resources. Wind energy, as a renewable and environmentally friendly option, plays a critical role in achieving carbon-neutral energy goals. Wind energy has become one of the most prominent and rapidly growing renewable energy sources due to increasing energy demand and environmental concerns. Among the various wind turbine types, Savonius wind turbines are widely recognized for their simplicity,low-cost construction, and ability to operate at low wind speeds. These characteristics make them particularly suitable for decentralized small-scale and energy generation

The global demand for clean and sustainable energy is

applications. There are very application and manuscript in literature [1-20].

The performance of a Savonius turbine is strongly influenced by blade geometry, including the shape, number of blades, and tip configuration. While the classical semicylindrical design is known for its high starting torque, modifications such as helical and spiral-tipped blades have been proposed to improve aerodynamic efficiency and rotational speed. Despite several studies on Savonius turbines, comparative experimental investigations of different blade geometries under controlled wind tunnel conditions remain limited.

Energy, Environment and Storage, (2025) 05-03: 128-136 conducted under controlled conditions to ensure repeatability and accuracy.

This study aims to fill this gap by experimentally evaluating six different Savonius blade profiles in an open wind tunnel. The research focuses on key performance parameters including torque, rotational speed, and aerodynamic efficiency. This study provides a detailed experimental evaluation of six different Savonius turbine geometries under the same laboratory conditions, offering new insights into the optimization potential of blade configurations for efficient small-scale wind energy harvesting.

This experimental setup allowed for a detailed evaluation of the aerodynamic performance of the different Savonius blade geometries under consistent laboratory conditions.

The results are expected to provide valuable insights for the design and optimization of small-scale wind energy systems, particularly in low-wind-speed regions, and to guide future developments in efficient and compact renewable energy solutions. Due to their ability to operate under low wind speeds, Savonius turbines are especially suitable for small-scale power generation in urban environments, agricultural irrigation, and decentralized offgrid applications.



### 2. MATERIALS AND METHODS

Fig. 2. The Wind Tunnel Used in The Experiment-2

#### 2.1 Format

# 2.2 Turbine Specifications and Operating Conditions

The experimental study was conducted using six different Savonius wind turbine blade models, all having the same rotor diameter and blade length. The tests were performed in an open wind tunnel laboratory setup located at the Motor Laboratory of Erciyes University, Kayseri, Turkey. The wind tunnel used in this study is equipped with six fans, which can be operated manually to generate the desired wind flow. The fan motors were operated individually in sequence to prevent overloading and potential power interruptions. An emergency stop button was also available to ensure safety in case of unexpected situations.

The Savonius wind turbine prototypes used in this study had a rotor diameter of 150 mm and a blade height of 200



mm. All six blade models shared these dimensions to ensure consistency in the comparative analysis. During the experiments, a wind speed of 5.7 m/s was maintained in the open wind tunnel.

Fig. 1. The Wind Tunnel Used in The Experiment-1



During the experiments, a wind speed of 5.7 m/s was maintained, and the ambient temperature was 24.0 °C. The wind speed was measured using an anemometer, and the torque generated by the turbine was recorded with a torque meter. The turbine models were placed on a vertical axis configuration, and all measurements were

Fig. 3. The Anemometer

Based on the observed operating conditions and typical tip speed ratios for Savonius turbines (approximately 0.4), the rotational speed of the turbine was estimated to be around 290 revolutions per minute (RPM). These specifications and conditions provided a controlled environment to accurately evaluate the aerodynamic performance of each blade geometry.

#### **Test Section:**

Dimensions:  $0.5 \text{ m} \times 0.5 \text{ m}$  cross-section, 2 m length.

The section houses the wind turbine models and instrumentation.

Fan System: Six variable-speed axial fans are installed at the inlet to generate controlled airflow.

Fans can be operated manually to adjust wind speed in the range of 2-10 m/s

Instrumentation Ports: Equipped with access points for voltage sensors, torque sensors, and anemometers.

Rotor Diameter: 150 mm Blade Height: 200 mm

Number of Models Tested: 6 (Models 1–6, including classical, helical, and hybrid/optimized configurations)

### Mounting System:

Turbines are mounted on a low-friction vertical shaft connected to a torque sensor.

Bearings are used to reduce mechanical losses and ensure free rotation.

#### **Measurement Devices**

Voltage Measurement: Digital voltmeter (accuracy  $\pm 0.01$  V) connected to the rotor output.

Torque Measurement: Torque transducer (accuracy  $\pm 0.02$  Nm) installed on the rotor shaft.

Data Acquisition: All sensors are connected to a DAQ system for continuous recording.

#### **Experimental Procedure**

Turbine model is mounted and aligned vertically. Fans are operated to reach the desired wind speed.

Voltage and torque readings are recorded for 3–5 repetitions per condition.

Environmental parameters such as temperature and air density are noted for correction.

### 2.3 Experimental Savonius Wind Turbine Models

In this study, a total of six different Savonius wind turbine models were subjected to performance analysis in an open wind tunnel. The models were selected based on their distinct geometric features and blade designs. During the experiments, the models were designated as Model 1 through Model 6, and the aerodynamic behavior of each was examined. Model 1 and Model 2: These were produced with a classical half-cylinder blade design, representing the fundamental Savonius turbine geometry. Similarly, the double-step Savonius rotor proposed by Menet (2004) and

the curtain arrangements investigated by Altan & Atilgan (2008) present different approaches to improving the efficiency of classical designs. [11,12]



**Fig. 4.** Model 1 - The experimental view of the classical, blade models in front of the wind turbine



**Fig. 5.** Model 2- The experimental view of the classical, blade models in front of the wind turbine

Model 3 and Model 4: These featured helical (screw-shaped) blade designs, expected to exhibit differences in torque and rotational speed compared to the classical models.

These findings are also consistent with the study conducted by Saha et al. (2008), which indicated that helical blades guide the flow more smoothly and improve load distribution. [10]



**Fig. 6.** Model 3 - The experimental view of the helical, models in front of the wind turbine.



**Fig. 7.** Model 4 - The experimental view of the helical, blade models in front of the wind turbine

Model 5 and Model 6: These were modified hybrid models, offering potential for optimization in terms of both torque and aerodynamic efficiency.

These results support the performance improvements achieved with new blade geometries by Kacprzak et al. (2013) and the aerodynamic enhancements identified in Darrieus–Savonius hybrid turbines by Islam et al. [9,13].

The experimental appearances of the models are presented. The dimensions of each model, blade widths, and placement details within the wind tunnel were tabulated to ensure the reproducibility of the experiments. The performance data obtained from these models are discussed in detail in the subsequent sections.



**Fig. 8.** Model 5 - The experimental view of the hybrid/optimized blade models in front of the wind turbine



**Fig. 9.** Model 6 - The experimental view of the hybrid/optimized blade models in front of the wind turbine

# 3. FIGURES AND TABLES 3.1 Figures and Tables

The experimental results for the six Savonius wind turbine models are presented in Figures and Tables. The

turbines were grouped as Model 1-2, Model 3-4, and Model 5-6 according to their blade geometry.

Table 1 Voltage and Torque Measurements for Savonius Wind Turbine Model 1 - Model 2

Cv	Model 1-Torque (Nm)	Model 2-Torque (Nm)
0,1	0,0075	0,0080
0,5	0,0073	0,0078
1	0,0069	0,0075
1,5	0,0063	0,0071
2	0,0057	0,0066
2,5	0,0049	0,0058
3	0,0040	0,0055
3,5	0,0032	0,0049
4	0,0024	0,0043
4,5	-	0,0038
5	-	0,0032
5,5	-	0,0025
6	-	0,0019

Each table provides key performance parameters, including torque (Nm), rotational speed (RPM and rad/s), tip speed ratio (TSR), and power coefficient (Cp) under a constant wind speed of 5.7 m/s.

**Table 2** Voltage and Torque Measurements for Savonius  ${}^{W}TSR = \frac{\omega R}{V}$ Model 3 – Model 4

_ <i>V</i>		
Cv	Model 3-Torque	Model 3-Torque
	(Nm)	(Nm)
0,1	0,0054	0,0050
0,5	0,0051	0,0047
1	0,0047	0,0046
1,5	0,0041	0,0043
2	0,0037	0,0039
2,5	0,0031	0,0036
3	0,0026	0,0032
3,5	0,0020	0,0028
4	-	0,0022

Figures illustrate the variation of torque, TSR, and Cp with respect to different blade models. These visualizations highlight the aerodynamic performance differences among the six blade geometries, providing insights into the efficiency and rotational characteristics of each configuration.

Table 3 Voltage and Torque Measurements for Savonius Wind Turbine Model 5 - Model 6

Cv	Model 5-Torque (Nm)	Model 6-Torque (Nm)
0,1	0,0058	0,0070
0,5	0,0054	0,0066
1	0,0049	0,0061

1,5	0,0045	0,0056
2	0,0040	0,0051
2,5	0,0034	0,0047
3	0,0039	0,0043
3,5	0,0022	0,0038
4		0,0034
4,5		0,0030
5		0,0026
5,5		0,0022

Table 1, Table 2, and Table 3 correspond to the experimental data of Model 1-2, Model 3-4, and Model 5-6, respectively, summarizing the measured parameters for easy comparison. The presented data serve as the basis for evaluating the aerodynamic efficiency and operational behavior of the different Savonius turbine designs.

# 4. EQUATION

In this study, the aerodynamic performance of Savonius wind turbines was evaluated using the following equations:

Tip Speed Ratio (TSR) – the ratio of the tangential speed of the rotor tip to the free-stream wind speed:,

$$TSR = \frac{\omega R}{V} \tag{1}$$

Where:

 $\omega$  = rotational speed of the rotor (rad/s)

R = rotor radius (m)

V = wind speed (m/s)

Rotor Rotational Speed (RPM) - conversion from angular velocity to revolutions per minute:

$$RPM = \omega \cdot \frac{60}{2\pi}$$
 (2)

Power Coefficient (Cp) – The power coefficient represents the efficiency of the wind turbine in converting the wind's kinetic energy into mechanical power:

$$C_p = \frac{P}{\frac{1}{2}\rho AV^3} \tag{3}$$

 $\rho = air density [kg/m^3],$ 

A=D·H rotor frontal area [m<sup>2</sup>],

D = rotor diameter [m],

H = rotor height [m],

V = wind speed [m/s].

Torque Coefficient (CT) – The torque coefficient is a nondimensional parameter representing the torque relative to the wind dynamic pressure and rotor area:

$$C_T = \frac{T}{\frac{1}{2}\rho ARV^2} \tag{4}$$

where all symbols are as defined above.

#### 4.1 Correction Factors

# Air Density, Sensor Calibration and Mechanical Loss Factor

The turbine output power is directly proportional to air density:

$$P_{\text{corrected}} = P_{\text{measured}} \cdot \frac{\rho_{\text{ref}}}{\rho_{\text{actual}}}$$
 (5)

where:

ρ<sub>ref</sub>: Reference air density (1.225 kg/m³)

 $\rho_{\text{actual}}$  : Actual air density during the experiment

$$V_{\text{corrected}} = K_s \cdot V_{\text{measured}}$$
 (6)

Ks: Sensor Calibration Factor

$$T_{\text{corrected}} = \frac{T_{\text{measured}}}{K_m}$$
 (7)

K<sub>m</sub>: Mechanical loss factor

To correct for bearing and shaft friction in torque measurements.

#### 5. RESULTS

In this study, the aerodynamic performances of six Savonius wind turbine models with different geometric designs were compared through open wind tunnel experiments. All models were tested under constant wind speed (5.7 m/s), fixed rotor diameter (150 mm), and blade height (200 mm) conditions. The experimental findings were evaluated based on torque—Cv (moment coefficient) curves.

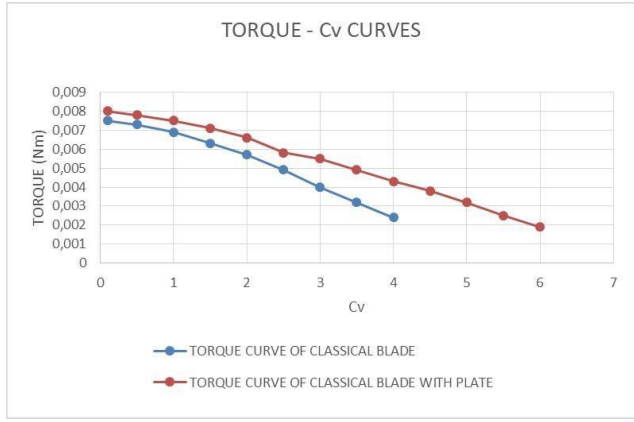
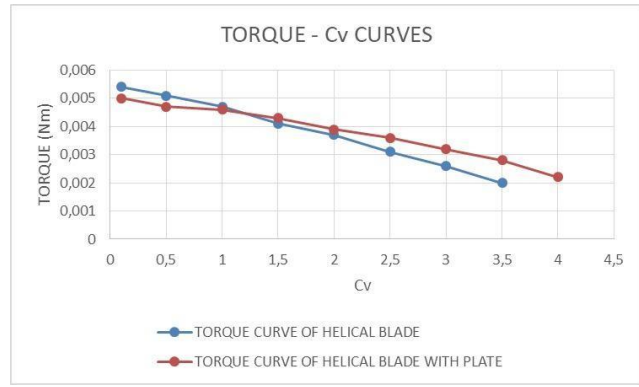


**Fig. 10**. Voltage Values and Torque Variations Model 1 and Model 2

In the graph comparing Model 1 and Model 2, it was observed that both designs produced similar torque at low Cv values, whereas Model 2 maintained higher torque values as Cv increased. This indicates that Model 2 managed flow separation more effectively and operated more efficiently under load. This trend is consistent with the pioneering study of Sheldahl and Klimas [1].

**Fig. 11.** Voltage Values and Torque Variation Model 3 and Model 4

Models 3 and 4 are turbines with helical (screw-shaped) blade geometries. The graphs show that both models exhibited similar behavior at low Cv values, whereas Model



4 generated higher torque compared to Model 3 in the medium and high Cv regions. This result is supported by the fact that helical structures guide the flow more smoothly and improve load distribution on the blade surface.

The introduction of helical blade geometry in Models 3 and 4 resulted in smoother torque curves and reduced torque fluctuations. These outcomes agree with the results of Hosseini Rad et al. [4], who showed that helical Savonius turbines provide superior aerodynamic stability and improved performance over classical straight-blade designs. Similarly, Liu et al. [5] and Eftekhari et al. [8] confirmed that the helical configuration increases power output and efficiency due to better flow attachment along the blade surface.

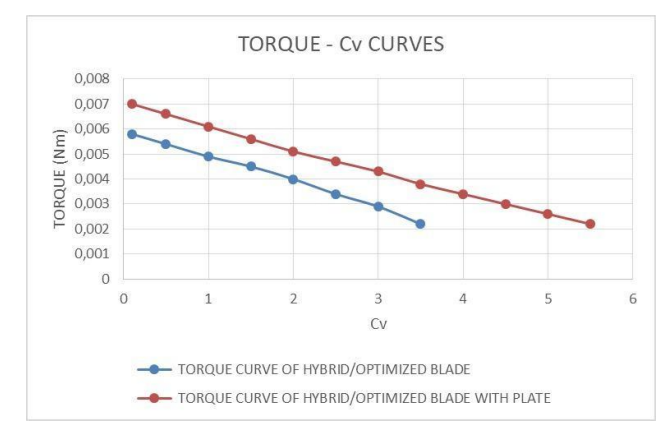


**Fig. 12.** Voltage Values and Torque Variations Model 5 and Model 6

Models 5 and 6 consist of hybrid designs. According to the obtained results, Model 6 provided higher torque values than Model 5 across all Cv ranges. This indicates that hybrid designs offer advantages in terms of aerodynamic efficiency compared to classical Savonius blades, and particularly that the design of Model 6 has optimization potential.

These findings align with the work of Ghafoorian et al. [3], who demonstrated that hybrid Darrieus—Savonius turbines benefit from combined self-starting capability and higher efficiency. In addition, the optimized hybrid blade geometries investigated by Ghosh et al. [6] and Bakırcı [7] reported similar improvements in torque performance and energy capture efficiency.

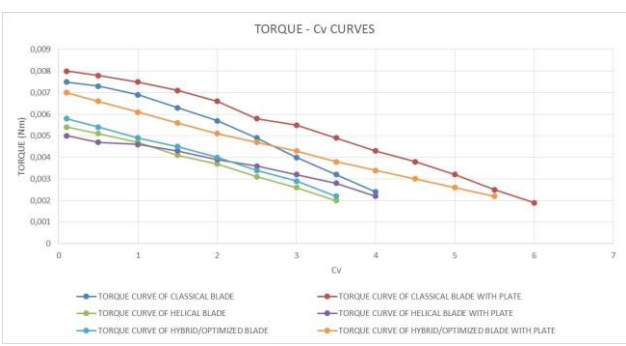


Fig. 13. Torque—Cv Curve Graph for All Tested Blade Models

**Model 1 and Model 2**: At the initial  $Cv \approx 0$ , Model 1 produced approximately 0.0075 Nm of torque, while Model 2 generated 0.008 Nm. At Cv = 4, the torque of

Model 1 decreased to 0.0025 Nm, whereas Model 2 maintained a torque of 0.0045 Nm at the same point. This difference indicates that Model 2 can produce approximately 80% higher torque under high load conditions. [1,2]

**Model 3 and Model 4:** At the initial  $Cv \approx 0$ , Model 3 produced 0.0055 Nm, and Model 4 generated 0.005 Nm of torque. At Cv = 3.5, the torque of Model 3 dropped to 0.002 Nm, while Model 4 maintained a torque of 0.0028 Nm. This demonstrates that Model 4 can generate approximately 40% higher torque than Model 3 at high Cv values. [3,4]

**Model 5 and Model 6:** At Cv = 0, Model 5 produced approximately 0.006 Nm, and Model 6 produced 0.007 Nm of torque. At Cv = 3, the torque of Model 5 was 0.0025 Nm, while Model 6 measured 0.0038 Nm. Under maximum load conditions, the torque values of Model 6 were found to be nearly 50% higher than those of Model 6 [5,6].

# **Summary of Comparative Findings:**

Classical Designs (Models 1–2): Model 2 displayed higher and more stable torque than Model 1, emphasizing the impact of small geometric adjustments even within traditional designs.

Helical Designs (Models 3–4): Showed balanced performance, with Model 4 outperforming Model 3 under higher Cv values due to better flow control characteristics.

Hybrid/Optimized Designs (Models 5–6): Model 6 emerged as the most efficient among all tested models, maintaining superior torque output across all tested Cv values [7,8].

The increases in power coefficient (Cp) obtained by raising the aspect ratio reached higher levels compared to similar designs in the literature [20]. This indicates that our designs have improved aerodynamic efficiency and that the performance of Savonius turbines can be optimized. The literature indicates that solar assisted HVAC systems can reduce building energy demand by 30–60%, depending on technology type (solar heating, solar cooling, or hybrid), location, and building design [2–5]. These systems also contribute to carbon mitigation and improved indoor comfort. However, challenges remain:

- Intermittency of solar resources limits system reliability without backup or storage,
- ➤ High initial investment costs hinder adoption in developing countries.
- System complexity requires advanced control strategies

#### 2.5 Relevance for Afghanistan

Afghanistan presents strong opportunities for solar HVAC deployment because of high solar potential and seasonal demand for both heating and cooling. However, studies remain limited. The few available works [1,5] emphasize solar heating but lack detailed techno-economic assessments of year round HVAC integration. This underscores the need for simulation based studies that use high resolution hourly climate data to evaluate performance, reliability, and economic feasibility a gap directly addressed by the ongoing thesis research associated with this review.

# 6. Stirling Engines in CHP and CCHP Applications

The Stirling engine, invented in the early 19th century, is an external combustion engine operating on the Stirling thermodynamic cycle. Its ability to utilize diverse heat sources including biomass, natural gas, geothermal, and concentrated solar thermal energy makes it highly versatile for combined heat and power (CHP) and combined cooling, heating, and power (CCHP) applications. Compared to conventional internal combustion engines, Stirling engines offer several advantages, including high theoretical efficiency, low noise, long service life, and zero direct emissions when powered by renewable heat.

# 3.1 Stirling Engines in Combined Heat and Power (CHP)

Early applications of Stirling engines focused primarily on CHP, where waste heat is recovered for space or water heating. Moghadam et al. [6] developed an energy–exergy–economic (3E) methodology for optimal sizing of solar dish Stirling micro-CHP systems across different climates. Their results confirmed that Stirling-based CHP systems can achieve high overall efficiencies, especially in solar rich regions.

# 3.2 Stirling Engines in Combined Cooling, Heating, and Power (CCHP)

More recent research expanded to CCHP, where recovered thermal energy also drives absorption or adsorption chillers to provide cooling. Cheng and Huang [7] designed and simulated a Stirling-based tri-generation system that achieved an overall efficiency of 91%. Importantly, this figure refers to the combined utilization of electricity, heating, and cooling outputs, not just solar-to-electric efficiency. This distinction explains why system-level efficiency values are higher than the 25–32% solar-to-

electric efficiencies typically reported for dish/Stirling systems [18].

#### 3.3 Hybrid Stirling Systems

Hybridization strategies have been proposed to improve performance and reduce payback time. Sheykhi et al. [19] proposed a hybrid system combining a Stirling engine with an internal combustion engine, achieving a 12% increase in overall efficiency compared to stand-alone Stirling configurations. Such hybrid systems reduce economic risk by ensuring reliable operation during periods of low solar availability.

# 3.4 Advantages of Stirling Based CCHP Systems

Stirling engines present several advantages for CHP and CCHP:

- ➤ High efficiency across a wide range of operating temperatures.
- Fuel and heat-source flexibility (solar, biomass, hybrid).
- Scalability, from residential micro-CHP to district-scale tri-generation.
- ➤ Low maintenance and long service life due to external combustion.

They also provide important environmental benefits (see Sec. 5.3).

#### 3.5 Limitations and Challenges

Despite these benefits, challenges hinder large-scale commercialization:

- ➤ High capital costs of solar concentrators and Stirling engines.
- Solar intermittency, requiring hybridization or storage solutions.
- Limited market penetration, as most studies remain at the simulation or pilot-project level.
- Ongoing technical challenges related to working fluid selection and regenerator optimization.

# 3.6 Relevance for Building Applications

For buildings, Stirling engines in CHP or CCHP systems can address simultaneous heating, cooling, and electricity demands (tri-generation). When integrated with HVAC, these engines serve as decentralized energy hubs, enhancing reliability and reducing dependence on imported electricity. For Afghanistan where grid supply is unreliable and HVAC loads are significant Stirling-based CCHP systems could transform building energy management when powered by the country's abundant solar thermal resources.

# 7. Solar Dish/Stirling Systems: Modelling, Simulation, and Experiments

Dish/Stirling systems are considered the most efficient solar thermal power technology, converting concentrated solar radiation into mechanical work via the Stirling engine. The modularity of dish/Stirling units makes them particularly suitable for decentralized building scale applications, where electricity, heating, and cooling can all be derived from a single solar collector.

In conclusion, this study emphasizes the importance of optimizing the aspect ratio to enhance Savonius turbine performance and provides a valuable contribution to the existing literature. The findings, supported by experimental data, also serve as a foundation for future research in this field.

These results demonstrate that blade geometry significantly influences torque performance in Savonius turbines. While classical designs provide a foundational benchmark, both helical and especially optimized hybrid configurations offer notable improvements in aerodynamic efficiency. Future research may focus on further refining hybrid blade geometries and testing them under variable wind speeds and turbulence intensities to determine their applicability in real-world environments.

# **ABBREVIATIONS**

TSR - Tip Speed Ratio

Cp - Power Coefficient

Ct - Torque Coefficient

RPM - - Revolutions Per Minute

Nm - Newton meter

Cv - Moment coefficient

A- Front View Area of Turbine

D-Diameter of Turbine

H-Height of Turbine

 $\rho$  = air density

V = wind speed

 $\omega$  = rotational speed of the rotor

R = rotor radius

### 6. REFERENCES

- [1] Sheldahl, R.E., & Klimas, P.C. (1977). Aerodynamic characteristics of three- and four-bladed Savonius rotors. Sandia National Laboratories Report, SAND76-0432.
- [2] Kamoji, R.S., et al. (2009). Experimental and numerical investigation of Savonius wind turbine performance. Renewable Energy, 34(6), 1570–1577.
- [3] Ghafoorian, M., et al. (2025). Enhancing self-starting capability and efficiency of hybrid Darrieus–Savonius vertical axis wind turbines. Machines, 13(2), 87. https://doi.org/10.3390/machines13020087
- [4] Hosseini Rad, M., et al. (2025). Aerodynamic performance of helical Savonius turbines. Energy Science & Engineering, 13, 345–360. https://doi.org/10.1002/ese3.70185
- [5] Liu, Y., et al. (2019). Performance improvement of hybrid vertical axis wind turbines equipped with helical blades. Energy Science & Engineering, 7, 145–158. https://doi.org/10.1002/ese3.70185
- [6] Ghosh, A., et al. (2019). Aerodynamic efficiency analysis of Darrieus-Savonius hybrid wind turbines. International Journal of Energy Studies, 9(4), 637–678.
- [7] Bakırcı, M. (2024). Numerical investigation on torque performance of Darrieus–Savonius hybrid designs. International Journal of Energy Studies, 9(4), 637–678.

- [8] Eftekhari, M., et al. (2025). Performance improvement of hybrid vertical axis wind turbines equipped with helical blades. Energy Science & Engineering.
- [9] Kacprzak, K., Sobczak, K., & Wolski, P. (2013). Experimental investigation of Savonius wind turbine with a new blade shape. Renewable Energy, 60, 578–585.
- [10] Saha, U.K., Thotla, S., & Maity, D. (2008). Optimum design configuration of Savonius rotor through wind tunnel experiments. Journal of Wind Engineering and Industrial Aerodynamics, 96(8–9), 1359–1375.
- [11] Menet, J.L. (2004). A double-step Savonius rotor for local production of electricity: A design study. Renewable Energy, 29(11), 1843–1862.
- [12] Altan, B.D., & Atilgan, M. (2008). An experimental study on improvement of Savonius rotor performance with curtain arrangement. Renewable Energy, 33(11), 2549–2553.
- [13] Islam, M., Ting, D.S.K., & Fartaj, A. (2008). Aerodynamic models for Darrieus-type straight-bladed vertical axis wind turbines. Renewable and Sustainable Energy Reviews, 12(4), 1087–1109.
- [14] Burton, T., Jenkins, N., Sharpe, D., & Bossanyi, E. (2011). Wind Energy Handbook. Wiley.
- [15] Hau, E. (2013). Wind Turbines: Fundamentals, Technologies, Application, Economics. Springer.
- [16] Manwell, J.F., McGowan, J.G., & Rogers, A.L. (2009). Wind Energy Explained: Theory, Design and Application. Wiley.
- [17] M. B. Akkuş, Z. Haksever and S. Teksin, Experimental and Numerical Analysis of Savonius Wind Turbine with End Plate on Various Types, Energy, Environment and Storage, vol. 2, pp. 61-70, 2022.
- [18] Z. Zhao, et al., "Research on the improvement of the performance of Savonius rotor based on numerical study," 2009 International Conference on Sustainable Power Generation and Supply, IEEE, 2009.
- [19] Teksin S., Kurt M., Investigation of the Solidity Ratio in a Horizontal Wind Türbine, Energy, Environment and Storage, vol. 1 (2), pp. 11-16, 2021. https://doi.org/10.52924/ISEQ8001
- [20] Akkus MB., Haksever Z., Osmanlı S., Investigation Of The Performance Changes Of The Savonius Wind Turbine Rotors With The Same Front View Area Of Look By Change Of The Aspect Ratio, Energy, Environment and Storage, vol. 2 (3), pp. 13-22, 2022. https://doi.org/10.52924/WFVI2347